

# Optimal object association from pairwise evidential mass functions

Nicole El Zoghby, Véronique Cherfaoui, Thierry Denoeux  
Heudiasyc, UMR CNRS 7253  
Université de Technologie de Compiègne, France  
nicole.el-zoghby@hds.utc.fr  
veronique.cherfaoui@hds.utc.fr  
thierry.denoeux@hds.utc.fr

**Abstract**—Object association is often a prior step in the data fusion process, especially for multiple objects tracking and multisensor data fusion. The approach introduced in this paper associates objects detected in a scene by two sensors, while modeling uncertainty using the Dempster-Shafer theory of belief functions. Sensor information is transformed into pairwise mass functions, which are combined using Dempster’s rule of combination. The result of this combination allows us to find the most plausible relation between two sets of objects by solving a linear programming problem. Experimental results with real data acquired from sensors embedded in intelligent vehicles are presented.

## I. INTRODUCTION

Object association is often a prior step in the data fusion process. This paper deals with the association of objects detected by two sensors in their area of interest. Sensors treat observations and provide information about objects such as number of detected objects, kinematic information (position, velocity), identification information (status, class, dimensions, etc.). Associating objects is a difficult problem since the number of objects in the scene is usually unknown and data provided by sensors can be uncertain and incomplete (with possible false alarms and non detections).

Many papers have dealt with this problem in order to associate objects perceived by different sensors or by the same sensor at different times. Classical data association methods are described in several books, such as Bar-Shalom and Fortmann [1] and Blackman and Popoli [2]. The NN (Nearest Neighbor), GNN (Global Nearest Neighbor), PDA (Probabilistic Data Association), JPDA (Joint Probabilistic Data Association) and MHT (Multi Hypothesis Tracking) methods are the main techniques associating observations with predictions for objects tracking. Some of them are dedicated to multiple sensors application called track-to-track association [3], [4]. Most of these methods require a probability measure to evaluate different hypotheses. These different methods, and others [5], [6], differ in their complexity as well as their ability to manage uncertainty and to handle ambiguities in the associations.

In this paper, we propose a formalization of the association problem using belief functions, in order to model uncertainties related to the object detector (the sensor) and to occlusion issues. Our method finds the most plausible relation between two sets of objects, such that each object in one set is matched with at most one object in the other set.

Several researchers have previously investigated this problem in the belief function framework. In [7], the authors present a method that determines the presence of different objects observed by different sensors. They use the degree of conflict to solve the problem of data association and apply their procedure to the detection of submarines. A method based on belief functions for data association for multiple target tracking problems was proposed in [8]. Schubert in [9] manages inconsistent intelligence as a preprocessing step to information fusion. Several techniques have been proposed for associating perceived objects and known objects for object tracking applications. Gruyer and Cherfaoui [10], based on [11], have developed an algorithm for multi-object association. To make a decision, they remove the ambiguity and provide heuristically a “good” solution for multi-object tracking. Mercier et al. [12], based on previous work by Rombaut [13] and Gruyer et al. [14], present a method that deals with object appearance and disappearance. They associate objects detected at time  $t$  with known objects (or tracks) at previous time. Their method takes into account two points of view: perceived and known objects. It is based on the similarity between object positions. However, this method is very time-consuming and it lacks a fundamental symmetry property, as it may give different results if the sets of known and perceived objects are interchanged. Ristic and Smets [15] proposed a method to associate objects based on information about their class.

In this paper, we are interested in associating mobile objects by taking into account all the available attributes such as position, velocity and class, together with their uncertainties. As in [13], [14], [12], dissimilarities between object attributes are considered as pieces of evidence and formalized as pairwise mass functions  $m_{ij}$  regarding the association of any pair of objects  $(e_i, f_j) \in E \times F$ , where  $E$  and  $F$  denote the two sets of objects to be associated. Based on this information, we show that the problem of finding the most plausible relation between  $E$  and  $F$  can be formalized as a binary linear program and solved very efficiently.

This paper is organized as follows. Belief functions are recalled in Section II. In Section III, we present our new object association formalism using belief functions. Then, the computation of mass functions from object attributes is explained in Section IV. Experimental results are presented in Section V. Finally, Section VI concludes the paper.

## II. BACKGROUND ON BELIEF FUNCTIONS

The theory of belief functions has two main components: equivalent representations of a body of evidence (in the form of mass, belief and plausibility functions), and a combination rule for combining independent items of evidence. These two components are reviewed in Subsection II-A and II-B, respectively.

### A. Representation of evidence

The theory of belief function is a framework for reasoning under uncertain based on the modeling of evidence [16]. More precisely, let us assume that we are interested in the value of some variable  $\theta$  taking values in a finite domain  $\Theta$ , called the *frame of discernment*. Uncertain evidence about  $\theta$  may be represented by a (normalized) *mass function*  $m$  on  $\Theta$ , defined as a function from the powerset of  $\Theta$ , denoted as  $2^\Theta$ , to the interval  $[0, 1]$ , such that  $m(\emptyset) = 0$  and

$$\sum_{A \subseteq \Theta} m(A) = 1. \quad (1)$$

Each number  $m(A)$  is interpreted as a *degree of belief* attached to the proposition  $\theta \in A$  and to *no more specific proposition*, based on some evidence.

To each normalized mass function  $m$ , we may associate belief and plausibility functions from  $2^\Theta$  to  $[0, 1]$  defined as follows:

$$Bel(A) = \sum_{B \subseteq A} m(B) \quad (2a)$$

$$Pl(A) = \sum_{B \cap A \neq \emptyset} m(B), \quad (2b)$$

for all  $A \subseteq \Theta$ . These two functions are linked by the relation  $Pl(A) = 1 - Bel(\overline{A})$ , for all  $A \subseteq \Theta$ . Each quantity  $Bel(A)$  may be interpreted as the degree to which the evidence *supports*  $A$ , while  $Pl(A)$  can be interpreted as the degree to which the evidence *is not contradictory* to  $A$ . The following inequalities always hold:  $Bel(A) \leq Pl(A)$ , for all  $A \subseteq \Theta$ . The function  $pl : \Theta \rightarrow [0, 1]$  such that  $pl(\theta) = Pl(\{\theta\})$  for all  $\theta \in \Theta$  is called the *contour function* associated to  $m$ .

### B. Combination of evidence

A key idea in DS theory is that beliefs are elaborated by aggregating different items of evidence. The basic mechanism for evidence combination is Dempster's rule of combination [16], defined as follows:

$$(m_1 \oplus m_2)(A) = \frac{1}{1 - \kappa} \sum_{B \cap C = A} m_1(B)m_2(C) \quad (3)$$

for all  $A \subseteq \Theta$ ,  $A \neq \emptyset$  and  $(m_1 \oplus m_2)(\emptyset) = 0$ , where

$$\kappa = \sum_{B \cap C = \emptyset} m_1(B)m_2(C) \quad (4)$$

is the *degree of conflict* between  $m_1$  and  $m_2$ . If  $\kappa = 1$ , there is a logical contradiction between the two pieces of evidence and they cannot be combined. Dempster's rule is commutative, associative, and it admits as neutral element the vacuous mass function, defined by  $m(\Theta) = 1$ .

Dempster's rule can be easily expressed in terms of contour functions: if  $pl_1$  and  $pl_2$  are the contour functions of two mass functions  $m_1$  and  $m_2$ , then the contour function of  $m_1 \oplus m_2$  is, using the same symbol  $\oplus$  as used for mass functions and contour functions

$$(pl_1 \oplus pl_2)(\theta) = \frac{pl_1(\theta)pl_2(\theta)}{1 - \kappa}, \quad (5)$$

for all  $\theta \in \Theta$ .

## III. OBJECT ASSOCIATION FORMALISM

### A. Association algorithm

We consider objects detected in a scene by two different sources  $S_1$  and  $S_2$ . Each sensor detects a set of objects denoted by  $E = \{e_1, e_2, \dots, e_N\}$  for  $S_1$  and  $F = \{f_1, f_2, \dots, f_M\}$  for  $S_2$ . We suppose that data are aligned in space and time, thanks to sensors calibration and evolution models. Mathematically, we are searching for a relation  $R \subseteq E \times F$  such that, for all  $i, j$  and  $k$ :

$$(e_i, f_j) \in R \text{ and } (e_i, f_k) \in R \Rightarrow j = k \quad (6a)$$

and

$$(e_i, f_k) \in R \text{ and } (e_j, f_k) \in R \Rightarrow i = j. \quad (6b)$$

Any such relation may be described by a matrix<sup>1</sup>  $R$  of size  $(n, p)$  such that  $R_{ij} = 1$  if  $(e_i, f_j) \in R$  and  $R_{ij} = 0$ .

We assume the available evidence about the association between the sets  $E$  and  $F$  to consist in  $NM$  mass functions  $m_{i,j}$ ,  $1 \leq i \leq N$ ,  $1 \leq j \leq M$ . Each  $m_{i,j}$  defined on the frame  $\Theta_{ij} = \{0, 1\}$  encodes a piece of evidence about a binary variable  $R_{i,j}$  that equals 1 if  $e_i$  and  $f_j$  correspond to the same entity, and 0 otherwise. The masses  $m_{ij}(\{1\})$  and  $m_{ij}(\{0\})$  quantify the support in the propositions  $R_{ij} = 1$  and  $R_{ij} = 0$ , respectively, while  $m_{ij}(\{0, 1\})$  is a mass that cannot be committed to any specific hypothesis because of ignorance. Typically,  $m_{i,j}$  is based on a measure of similarity between some attributes describing the objects, as will be shown in Section IV.

The key idea behind our approach is to express all the available evidence in the frame of discernment  $\mathcal{R}$ , i.e., the set of all possible matchings between  $E$  and  $F$  verifying (6a)-(6b). Assuming independence between the  $NM$  items of evidence, the  $NM$  mass functions can then be combined using Dempster's rule (3), and the plausibility of any relation  $R \in \mathcal{R}$  may be simply calculated.

Let  $\mathcal{R}_{ij}$  denote the set of relations that match objects  $e_i$  and  $f_j$ :

$$\mathcal{R}_{ij} = \{R \in \mathcal{R} | R_{ij} = 1\}. \quad (7)$$

Each mass function  $m_{ij}$  on  $\Theta_{ij} = \{0, 1\}$  may be expressed in  $\mathcal{R}$  by transferring the mass  $m_{ij}(\{1\}) = \alpha_{ij}$  to  $\mathcal{R}_{ij}$ ,  $m_{ij}(\{0\}) = \beta_{ij}$  to  $\mathcal{R}_{ij}$  and  $m_{ij}(\{0, 1\}) = 1 - \alpha_{ij} - \beta_{ij}$  to  $\mathcal{R}$ , where  $\mathcal{R}_{ij}$  denotes the complement of  $\mathcal{R}_{ij}$ . Let  $pl_{ij}$  denote the corresponding contour function. It has the following expression:

$$pl_{ij}(R) = \begin{cases} 1 - \beta_{ij} & \text{if } R \in \mathcal{R}_{ij}, \\ 1 - \alpha_{ij} & \text{otherwise,} \end{cases} \quad (8)$$

<sup>1</sup>By abuse of notation but without any risk of confusion, we use the same notation for the relation and its corresponding matrix.

for all  $R \in \mathcal{R}$ , which can be expressed more concisely as follows:

$$pl_{ij}(R) = (1 - \beta_{ij})^{R_{ij}}(1 - \alpha_{ij})^{1-R_{ij}}. \quad (9)$$

Let  $m$  denote the mass function on  $\mathcal{R}$  obtained by combining the  $NM$  mass functions using Dempster's rule. From (5), its contour function  $pl$  is proportional to the product of the  $NM$  mass functions  $pl_{ij}$ :

$$pl(R) \propto \prod_{i,j} (1 - \beta_{ij})^{R_{ij}}(1 - \alpha_{ij})^{1-R_{ij}}, \quad (10)$$

and its logarithm is

$$\ln pl(R) \propto \sum_{i,j} R_{ij} \ln(1 - \beta_{ij}) + (1 - R_{ij}) \ln(1 - \alpha_{ij}) + C, \quad (11)$$

where  $C$  is a constant.

The most plausible relation  $R^*$  can thus be found by solving the following linear optimization problem:

$$\max \sum_{i,j} w_{ij} R_{ij} \quad (12a)$$

with

$$w_{ij} = \ln \frac{1 - \beta_{ij}}{1 - \alpha_{ij}}, \quad (12b)$$

subject to

$$\sum_{j=1}^M R_{ij} \leq 1 \quad \forall i \quad (12c)$$

$$\sum_{i=1}^N R_{ij} \leq 1 \quad \forall j \quad (12d)$$

$$R_{ij} \in \{0, 1\} \quad \forall (i, j), \quad (12e)$$

where constraints (12c) and (12d) are related to Equations (6a) and (6b), respectively. The basic mathematical structure of the problem makes constraint (12e) unnecessary, as there will always be an optimal linear programming solution in which all  $R_{ij}$ 's are either 0 or 1.

### B. Comparison with the Mercier's approach

Following previous work by Rombaut [13] and Gruyer et al. [14], Mercier et al. [12] attempted to find a relation between two sets of objects  $E$  and  $F$  (referred to as "known" and "perceived" objects, respectively), based on pairwise mass functions, as considered in this paper. Their approach involves computing, for each known object, a mass function over the set of all perceived objects. They then propose an algorithm trying to find an association with maximum pignistic probability [17]. However, the method involves enumerating  $(N+1)^M$  possible associations and thus quickly becomes intractable when more than a few objects have to be matched. Furthermore, it may yield different results if the sets of known and perceived objects are interchanged, which suggest that there is a fundamental flaw in the approach.

To illustrate this point, let us consider the following very simple example from [12]. Assume that we have  $N = 1$ ,  $M = 2$  and the following weights (with our notations):

$$\alpha_{11} = 0.5, \quad \beta_{11} = 0, \quad \alpha_{12} = 0.7, \quad \beta_{12} = 0.3.$$

By adopting the "known objects" points of view, Mercier et al. find the following relation  $R = R_1 = [0 \ 1]$ , meaning that object  $e_1$  is associated with object  $f_2$ . In contrast, when adopting the "perceived object" point of view, they find  $R = R_2 = [1 \ 0]$ , i.e., object  $e_1$  is associated with object  $f_1$ . Using (10), we can check that  $pl(R_1)/pl(R_2) = 4.67$ , meaning that  $R_1$  is much more plausible than  $R_2$ . Actually, it is the unique solution found by solving the optimization problem presented above.

## IV. COMPUTATION OF PAIRWISE MASS FUNCTIONS FROM OBJECT ATTRIBUTES

Our aim is to associate objects using all available attributes, including position, velocity, class and possibly others. Let  $m_{ij}^p$ ,  $m_{ij}^v$  and  $m_{ij}^c$  denote, respectively, the pairwise mass functions obtained from position, velocity and class information. These mass functions will be combined using Dempster's rule (3):

$$m_{ij} = m_{ij}^p \oplus m_{ij}^v \oplus m_{ij}^c. \quad (13)$$

The computation of  $m_{ij}^p$ ,  $m_{ij}^v$  and  $m_{ij}^c$  is explained below.

### A. Position and velocity

Let us first consider how knowledge about the relative position of two objects can be expressed as a pairwise mass function  $m_{ij}^p$ . Let  $d_{ij}$  denote the (Euclidean, Mahalanobis or other) distance between the positions objects  $e_i$  and  $f_j$ . It is clear that a single object cannot have two distinct positions and, conversely, two objects cannot occupy exactly the same position. Consequently, a small value of  $d_{ij}$  supports the hypothesis  $R_{ij} = 1$ , while a large value of  $d_{ij}$  supports the hypothesis  $R_{ij} = 0$ . Depending on the sensor reliability, a fraction of the unit mass should also be assigned to  $\Theta_{ij} = \{0, 1\}$ . This line of reasoning justifies a mass function  $m_{ij}^p$  of the form:

$$m_{ij}^p(\{1\}) = \alpha \varphi(d_{ij}) \quad (14a)$$

$$m_{ij}^p(\{0\}) = \alpha (1 - \varphi(d_{ij})) \quad (14b)$$

$$m_{ij}^p(\Theta_{ij}) = \alpha, \quad (14c)$$

where  $\alpha \in [0, 1]$  is a degree of confidence in the information and  $\varphi$  is a decreasing function taking values in  $[0, 1]$ . For instance, the following form may be chosen for  $\varphi$ :

$$\varphi(d) = \exp(-\gamma d), \quad (15)$$

where  $\gamma$  is a positive coefficient.

Let us now consider velocity. Let  $d'_{ij}$  denote the distance between the velocities of objects  $e_i$  and  $f_j$ . Here, this piece of evidence does not have the same interpretation as the previous one: a large value of  $d'_{ij}$  supports the hypothesis  $R_{ij} = 0$ , whereas a small value of  $d'_{ij}$  does not support specifically  $R_{ij} = 1$  or  $R_{ij} = 0$ , as two distinct objects may have similar velocities. Consequently, the following form of the mass function  $m_{ij}^v$  induced by  $d'_{ij}$  seems appropriate:

$$m_{ij}^v(\{0\}) = \alpha' (1 - \psi(d'_{ij})) \quad (16a)$$

$$m_{ij}^v(\Theta_{ij}) = 1 - \alpha' (1 - \psi(d'_{ij})), \quad (16b)$$

where, as before,  $\alpha' \in [0, 1]$  is a degree of confidence in the information and  $\psi$  is a decreasing function taking values in  $[0, 1]$ . This function can be chosen to have the same form as (15), possibly with a different coefficient  $\gamma'$ .

## B. Class information

Class information can be exploited as evidence about object association. Clearly, two objects from different classes cannot be matched. Ristic and Smets in [15] make a much stronger assumption and postulate that two objects belonging to the same class should be considered as identical. This assumption is obviously not tenable when the number of classes is smaller than the number of objects. We will not make this assumption here.

Let  $m_i$  and  $m_j$  denote the mass functions on  $\Omega = \{\omega_1, \dots, \omega_c\}$ , quantifying our knowledge about the class of each object  $i$  and  $j$ . Let  $S_{ij}$  denote the proposition that objects  $i$  and  $j$  belong to the same class. As shown in [18], the plausibility of  $S_{ij}$  and its negation  $\overline{S}_{ij}$  have the following expressions:

$$\begin{aligned} pl_{ij}(S_{ij}) &= 1 - \sum_{A \cap B = \emptyset} m_i(A)m_j(B) \\ &= 1 - \kappa_{ij} \\ pl_{ij}(\overline{S}_{ij}) &= 1 - \sum_{k=1}^c m_i(\{\omega_k\})m_j(\{\omega_k\}) \\ &= 1 - \gamma_{ij}, \end{aligned} \quad (17)$$

where  $\kappa_{ij}$  is the degree of conflict between  $m_i$  and  $m_j$ . The corresponding function  $\mu_{ij}$  on  $\Omega_{ij} = \{S_{ij}, \overline{S}_{ij}\}$  has the following expression:

$$\begin{aligned} \mu_{ij}(\{S_{ij}\}) &= \gamma_{ij} \\ \mu_{ij}(\{\overline{S}_{ij}\}) &= \kappa_{ij} \\ \mu_{ij}(\Omega_{ij}) &= 1 - \gamma_{ij} - \kappa_{ij}. \end{aligned} \quad (18)$$

Now, the following implication holds:  $\overline{S}_{ij} \Rightarrow R_{ij} = 1$ . In contrast, nothing can be said about  $R_{ij}$  whenever  $S_{ij}$  holds. Consequently, expression  $\mu_{ij}$  in the frame  $\Theta_{ij}$  yields the following mass function  $m_{ij}^c$ :

$$\begin{aligned} m_{ij}^c(\{0\}) &= \kappa_{ij} \\ m_{ij}^c(\Theta_{ij}) &= 1 - \kappa_{ij}. \end{aligned} \quad (19)$$

## V. RESULTS

Our approach was experimented on real data. Objects were detected by two different sensors: a Mobileye ( $S_1$ ) and a Lidar Ibeo Alasca XT ( $S_2$ ). The Mobileye sensor uses mono camera only; it has pattern recognition capabilities based on image processing and optic flow analysis. This sensor provides information about objects such as: id, status, type, position, age and width. The Ibeo Alasca-XT Laser scanner supports four scan layers. We used the information processing system developed by Fayad et al. [19], [20]. This system detects and recognizes pedestrians from laser scanner information.

Results were evaluated on a sequence of 58 frames with an average of 8 objects in each frame. Our approach was applied to all the objects detected in the scene. Figure 1 shows an example of object detection using  $S_2$ . The figure on the right is just an image projection used for the visualization of objects on the road (it projects objects between the two red lines). It shows the detection of two objects. The figure on the left represents the circles encompassing all the detected objects. In this experiment, only two attributes were used: position and class.

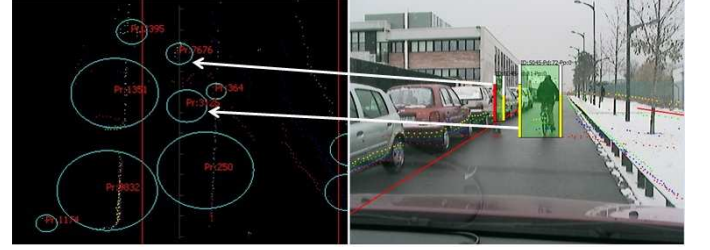


Fig. 1: Object detection system. The figure on the right is an image projection used for the visualization of two objects on the road. The left figure shows the circles encompassing all the detected objects.

TABLE I:  $m_{ij}^p$

$m_{ij}^p(\{1\})$	$f_1$	$f_2$	$f_3$	$f_4$
$e_1$	0.45	0.01	0.32	0.68
$e_2$	0.71	0.02	0.34	0.39
$e_3$	0.01	0.73	0.02	0.01
$m_{ij}^p(\{0\})$	$f_1$	$f_2$	$f_3$	$f_4$
$e_1$	0.45	0.89	0.58	0.22
$e_2$	0.18	0.88	0.56	0.51
$e_3$	0.9	0.17	0.88	0.89

### A. Computation of mass function

The Mahalanobis distance between each pair objects was computed as follows:

$$d_{ij} = \sqrt{\left( \begin{array}{c} x_i - x_j \\ y_i - y_j \end{array} \right)^T (P_i + P_j)^{-1} \left( \begin{array}{c} x_i - x_j \\ y_i - y_j \end{array} \right)} \quad (20)$$

where  $(x, y)$  denote the coordinates of the center of each object, and  $P$  is the covariance matrix. The mass function  $m_{ij}^p$  was computed using (14) with  $\alpha = 0.9$  and  $\gamma = 0.1$ .

Sensor  $S_2$  provides a mass function  $m_i$  about the class of each object  $i$ . The set of classes is  $\Omega_2 = \{P, NP\}$ , where  $P$  and  $NP$  represent pedestrian and non pedestrian, respectively. Sensor  $S_1$  provides the type of each object but it does not compute any corresponding confidence; the set of classes for this sensor  $\Omega_1 = \{Vehicle, Pedestrian, Truck, Bike, Bicycle\}$ , it is thus a refinement of  $\Omega_2$ . Consequently, evidence expressed in  $\Omega_1$  can easily be expressed in  $\Omega_2$ . A mass function  $m_j$  encoding the class information provided by  $S_2$  was constructed by assigning the mass 0.9 to  $\{P\}$  or  $\{NP\}$  depending on the sensor's decision, and a mass 0.1 to  $\{P, NP\}$ .

Mass functions  $m_i$  and  $m_j$  were used to compute  $m_{ij}^c$  using (19).

### B. Example

In this section, we detail an example presented in Figure 2, where sensor  $S_1$  detects three objects shown in Figure 2b (two pedestrians ( $e_1, e_2$ ) and one car  $e_3$ ) and  $S_2$  detects four objects shown in Figure 2c (two pedestrians ( $f_1, f_4$ ), one car  $f_2$  and a false detection  $f_3$ ). The results can be projected on images through the calibration method introduced in [21]. The corresponding position mass function is presented in Table I.

Sensor  $S_2$  provides the following class mass function:

TABLE II:  $m_{ij}^c$

$m_{ij}^c(\{0\})$	$f_1$	$f_2$	$f_3$	$f_4$
$e_1$	0	0.77	0	0
$e_2$	0	0.77	0	0
$e_3$	0.5	0	0.57	0.76
$m_{ij}^c(\Theta_{ij})$	$f_1$	$f_2$	$f_3$	$f_4$
$e_1$	1	0.23	1	1
$e_2$	1	0.23	1	1
$e_3$	0.5	1	0.43	0.24

TABLE III: Contour functions  $pl_{ij}$ . The two numbers on each cell are  $pl_{ij}(1)$  and  $pl_{ij}(0)$ .

$pl_{ij}$	$f_1$	$f_2$	$f_3$	$f_4$
$e_1$	0.55	0.02	0.41	0.78
	0.55	0.99	0.68	0.31
$e_2$	0.81	0.03	0.43	0.49
	0.28	0.99	0.66	0.6
$e_3$	0.05	0.82	0.05	0.02
	0.99	0.27	0.99	0.99

$$\begin{array}{lll}
 m_1(\{P\}) & = & 0.55 \\
 m_1(\{NP\}) & = & 0 \\
 m_1(\Omega) & = & 0.45 \\
 \\ 
 m_3(P) & = & 0.63 \\
 m_3(\{NP\}) & = & 0 \\
 m_3(\Omega) & = & 0.37
 \end{array}
 \quad
 \begin{array}{lll}
 m_2(\{P\}) & = & 0 \\
 m_2(\{NP\}) & = & 0.86 \\
 m_2(\Omega) & = & 0.14 \\
 \\ 
 m_4(\{P\}) & = & 0.84 \\
 m_4(\{NP\}) & = & 0 \\
 m_4(\Omega) & = & 0.16
 \end{array}$$

After combination, we obtain the mass functions  $m_{ij}^c$  shown in Table II. These mass functions were then combined using the Dempster's rule and the contour functions shown in Table III were then computed using (9).

The most plausible relation  $R^*$  in this case is found to be:

$$R^* = \begin{bmatrix} 0 & 0 & 0 & 1 \\ 1 & 0 & 0 & 0 \\ 0 & 1 & 0 & 0 \end{bmatrix}. \quad (21)$$

We can conclude that the pedestrians  $e_1$  and  $e_2$  detected by  $S_1$  are associated to the pedestrians  $f_4$  and  $f_1$  detected by  $S_2$ . The car  $e_3$  detected by  $S_1$  is associated to the car  $f_2$  detected by  $S_2$  and the false detection  $f_3$  of  $S_2$  is not associated. These results are shown in Figure 2d.

### C. Comparison with Mercier's approach

We tried to compare our results with those obtained using the method developed by Mercier et al. [12]. However, we were confronted to the combinatorial complexity of Mercier's method. For that reason, we filtered objects in order to decrease the size of the problem. We compared these two methods on 58 frames with three to five objects in each one. The results are similar in most cases. However, they differ when the class information is important. The performances can be assessed using precision and recall, defined as follows:

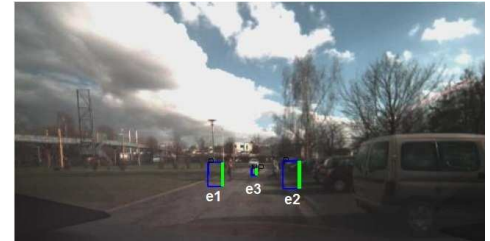
$$Precision = \frac{|\{\text{true pairs}\} \cap \{\text{matched pairs}\}|}{|\{\text{matched pairs}\}|} \quad (22)$$

$$Recall = \frac{|\{\text{true pairs}\} \cap \{\text{matched pairs}\}|}{|\{\text{true pairs}\}|}. \quad (23)$$

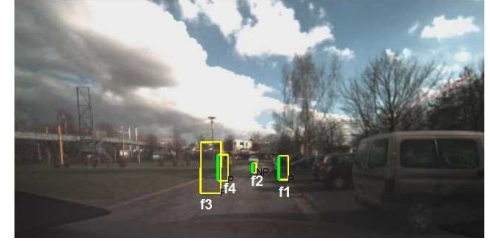
Precision is thus the proportion of matched pairs that really correspond to the same object, while Recall is the proportion of true pairs of objects that were matched correctly.



(a) The scene where we can see three objects: two pedestrians “P” and one car “C”.



(b) Objects detection with  $S_1$ , the green bar shows objects that are associated in Figure 2e.



(c) Objects detection with  $S_2$ , the green bar shows objects that are associated in Figure 2e.



(d) Laser detection bird view.



(e) Association results.

Fig. 2: Association between the two sensors  $S_1$  and  $S_2$ . Figure 2a shows the scene. Figure 2c presents the detection of four objects (two pedestrians, a car and a false alarm) with  $S_2$ . In Figure 2b, the Mobileye detects three objects (two pedestrians and a car). Figure 2d is a bird view of objects detected by  $S_2$ . Figure 2e shows the result of the association.

TABLE IV: Performance comparison

	Optimal approach	Mercier's approach
Average computing time (s)	0.0175	36.41
Time for $N = 3$ and $M = 10$ (s)	0.014	9.36
Precision	0.78	0.73
Recall	0.9	0.9

The results are summarized in Table IV.

#### D. Case of conflicting evidences

In order to explore conflicting evidences, we tested the association algorithm on simulated data, created by A. Houenou [4]. One vehicle  $V_0$  is equipped with two sensors:  $S_1$  (field of view :  $\text{maxrange} = 60m$  and  $\alpha = 45^\circ$ ) and  $S_2$  (field of view :  $\text{maxrange} = 100m$  and  $\alpha = 120^\circ$ ). It can detect other vehicles on the highway (up to 9 vehicles) as shown in figure 3. Each vehicle detected by  $V_0$  is characterized by its kinematic information (position and velocity), its covariance matrix and its class. We associate all the detected objects by  $S_1$  and  $S_2$  at each time step. In this simulation, we do not consider the occlusions in order to detect most of the objects on the road.

To evaluate the conflict, we calculate equation 12a by using the most plausible relation  $R^*$ , the result of the association, and we deduce the countour function  $pl$  as defined in eq. 10. Conflicting evidences will lead to a lower plausibility. We tested the scenario for 25s (the time step is 0.01) and we simulate different conflicting situations. The result of the plausibility is shown in figure 4. The plausibility is low between [5s,18s]. The plausibility equal to 1 refers to the cases where one sensor could not detect objects in its field of view, so there is no ambiguities in the association process.

Figure 6 presents the case at  $t = 4.8s$  where the plausibility is not low ( $pl = 0.18$ ) where  $S_2$  of  $V_0$  detects  $\{V_1, V_5\}$  while  $S_1$  detects  $\{V_1\}$ .  $V_1$  is associated to  $V_1$ .

In figure 5,  $S_2$  detects, at  $t = 17.3s$ , 7 objects:  $\{V_1, V_2, V_3, V_4, V_5, V_6, V_7\}$  while  $S_1$  detects, at the same time, 3 objects:  $\{V_1, V_2, V_7\}$ . The most plausible relation  $R^*$  in this case is found to be:

$$R^* = \begin{bmatrix} 1 & 0 & 0 & 0 & 0 & 0 & 0 \\ 0 & 1 & 0 & 0 & 0 & 0 & 0 \\ 0 & 0 & 0 & 0 & 0 & 0 & 1 \end{bmatrix}. \quad (24)$$

and  $pl$  is equal to 0.013. It is a low value that presents a high degree of conflict because other nearby vehicles are candidate for association, but it's shown that the association algorithm can find the most plausible solution in spite of the conflict.

## VI. CONCLUSION

In this paper, we have presented a new object association method within the belief function framework. Given two sets of objects, this method encodes attribute information provided by sensors into pairwise mass functions representing evidence about the possible matching of each pair of objects from both sets. These mass functions are combined using Dempster's rule of combination. The result of this combination is then used to find the most plausible relation between the two sets of objects. The optimal solution can be found by a linear programming

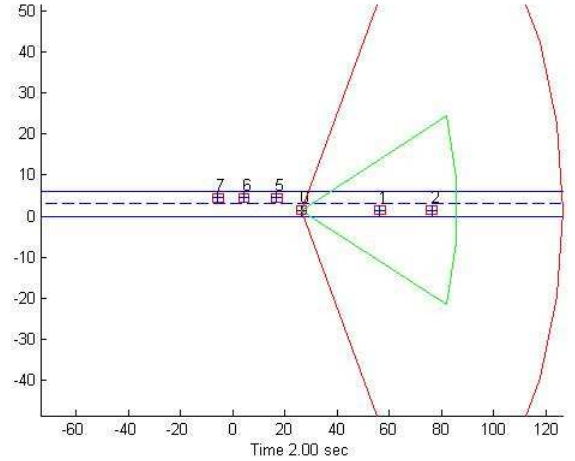


Fig. 3: Example of simulated data

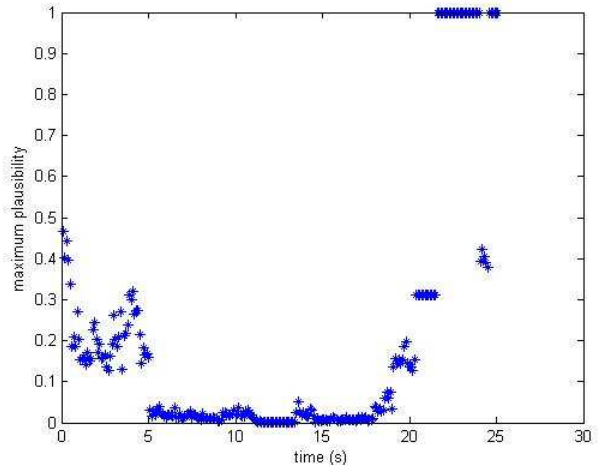


Fig. 4: Plausibility of  $R^*$

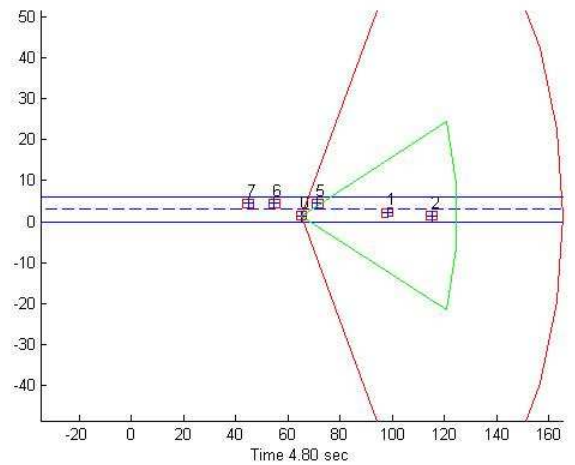


Fig. 5: Scenario at  $t=17.3s$

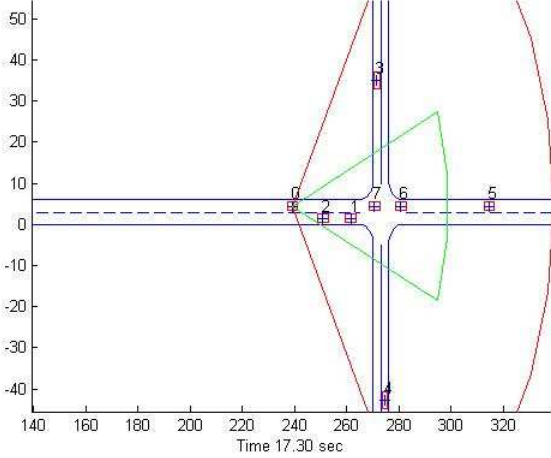


Fig. 6: Scenario at  $t=4.8s$

approach. This method is both optimal and much faster than the one recently introduced in [12] to solve the same problem. Our method has been validated by experiments with real data. It is being currently implemented as part of a distributed data fusion system for intelligent vehicles. Results will be reported in future publications.

#### ACKNOWLEDGMENT

This work was carried out in the framework of the Labex MS2T, which was funded by the French Government, through the program “Investments for the future” managed by the National Agency for Research (Reference ANR-11-IDEX-0004-02). The authors would like to thank G. Dherbomez, V. Fremont and A. Houenou for their contribution in the acquisition of data.

#### REFERENCES

- [1] Y. Bar-Shalom and T. Fortmann, *Tracking and data association*. Boston: Academic Press, 1988.
- [2] S. Blackman and R. Popoli, *Design and Analysis of Modern Tracking Systems*. Artech House, 1999.
- [3] L. Kaplan, Y. Bar-Shalom, and W. Blair, “Assignment costs for multiple sensor track-to-track association,” *IEEE Transactions on Aerospace and Electronic Systems*, pp. 655 – 677, April 2008.
- [4] A. Houenou, P. Bonnifait, V. Cherfaoui, and J. Boissou, “A track-to-track association method for automotive perception systems,” in *IEEE Intelligent Vehicles Symposium*, Alcal de Henares, Spain, June 3-7 2012, pp. 704–710.
- [5] K. Smith, “Reversible-jump Markov chain Monte Carlo multi-object tracking tutorial,” IDIAP Research Institute, Communication IDIAP-COM-06-07, 2006. [Online]. Available: <http://cvlab.epfl.ch/ksmith/RJMCMD.php>
- [6] R. Schubert, C. Adam, E. Richter, S. Bauer, H. Lietz, and G. Wanielik, “Generalized probabilistic data association for vehicle tracking under clutter,” in *Intelligent Vehicles Symposium*, Alcala de Henares, Spain, June 3-7 2012, pp. 962–968.
- [7] A. Ayoun and P. Smets, “Data association in multi-target detection using the Transferable Belief Model,” *International Journal of Intelligent Systems*, vol. 16, pp. 1167–1182, 2001.
- [8] N. Meghrebi, S. Ambellouis, O. Colot, and F. Cabestaing, “Multimodal data association based on the use of belief functions for multiple target tracking,” in *8th International Conference on Information Fusion (FUSION)*, Philadelphia, PA (USA), 2005, pp. 900–906.
- [9] J. Schubert, “Managing inconsistent intelligence,” in *3th Int. Conf. on Information Fusion*, Paris, France, 2000, pp. 4–10.
- [10] D. Gruyer and V. Cherfaoui, “Matching and decision for vehicle tracking in road situation,” in *IEEE/RSJ International Conference on Intelligent Robots and Systems IROS’99*, Kyongju, Korea, 17-21 October 1999, pp. 29–34.
- [11] M. Rombaut and V. Cherfaoui, “Decision making in data fusion using dempster-shafer’s theory,” in *3th IFAC Symposium on Intelligent Components and Instrumentation for Control Applications*, Annecy, France, 9-11 june 1997, pp. 375–379.
- [12] D. Mercier, E. Lefèvre, and D. Jolly, “Object association with belief functions, an application with vehicles,” *Information Sciences*, vol. 181, no. 24, pp. 5485–5500, December 2011.
- [13] M. Rombaut, “Decision in multi-obstacle matching process using the theory of belief,” in *Advances in Vehicle Control and safety, AVCS98*, Amiens, France, 1-3 july 1998, pp. 63–68.
- [14] D. Gruyer, C. Royère, R. Labayrade, and D. Aubert, “Credibilistic multisensor fusion for real time application, application to obstacle detection and tracking,” in *IEEE Int. Conf. on Advanced Robotics, ICAR’2003*, Coimbra, Portugal, June 30-July 3 2003, pp. 1462–1467.
- [15] B. Ristic and P. Smets, “Global cost of assignment in the TBM framework for association of uncertain id reports,” *Aerospace Science and Technology*, vol. 11(4), pp. 303–309, 2007.
- [16] G. Shafer, *A Mathematical Theory of Evidence*. Princeton University Press, 1976.
- [17] P. Smets and R. Kennes, “The transferable belief model,” *Artificial Intelligence*, vol. 66, pp. 191–234, 1994.
- [18] T. Denoeux and M.-H. Masson, “Evelus: Evidential clustering of proximity data,” *IEEE transactions on Systems, Man and Cybernetics B*, vol. 34(1), pp. 95–109, 2004.
- [19] F. Fayad and V. Cherfaoui, “Detection and recognition confidences update in a multi-sensor pedestrian tracking system,” in *Int. Conf. on Information Processing and Management of Uncertainty in knowledge-Based Systems, IPMU 2008*, Malaga, 2008, pp. 409–416.
- [20] F. Fayad, V. Cherfaoui, and G. Derbhomez, “Updating confidence indicators in a multi-sensor pedestrian tracking system,” in *IEEE Intelligent Vehicles Symposium IV2008*, Eindhoven, 2008, pp. 156–161.
- [21] V. Frémont, S. Rodriguez, and P. Bonnifait, “Circular targets for 3d alignment of video and lidar sensors,” *Advanced Robotics*, vol. 28, no. 18, pp. 2087–2113, September 2012.